IOP Conf. Series: Materials Science and Engineering **426** (2018) 012005 doi:10.1088/1757-899X/426/1/012005

Comparative study on theoretical and experimental evaluation of forming limit diagrams

G Béres[1], Z Weltsch[1] and M Tisza[2]

[1] John von Neumann University, Faculty of GAMF Engineering and Computer Science, Department of Materials Technology, Kecskemét¸ Hungary
[2] University of Miskolc, Faculty of Mechanical Engineering and Informatics, Institute of Materials Sciences & Technology, Miskolc-Egyetemváros, Hungary

E-mail: beres.gabor@gamf.uni-neumann.hu

Abstract. Forming limit diagrams (FLDs) are generally used to reflect the strain limits of sheet metal materials. These diagrams contain essential information for planning of high series stamping processes, however the experimental definition is still a difficult and time-consuming procedure. Five or more samples are needed to cover the different strain paths sufficiently, from pure shear ($\varepsilon_1 = -2\varepsilon_2$) up to biaxial stretch forming ($\varepsilon_1 = \varepsilon_2$), moreover the experimental detection of the onset of local necking depends on the capability of the measuring equipment and person. The determination of the measurement results is further complicated by the material and other influencing conditions, like strain path (deformation history), rolling direction, sheet thickness, temperature, measuring grid size, tool surfaces, friction and vibrations. All these things supports the development of clearly theoretical and semi-empirical models for defining FLDs. This paper presents a comparative study of some kind of well-known theoretical models and experimental FLDs of automotive dual phase (DP) thin sheets. The experimental determination was carried out by Nakajima tests on five different sample geometries. We used follow-up strain analysis on the cracked samples. The results highlighted that most of the theoretical and semi-empirical models can be appropriately used in the negative quadrant of the FLD despite of the effect of the friction. However, in the positive quadrant, there are some more visible deviations due to outer conditions like lubricant.

1. Introduction

Due to the importance of forming limit diagrams, many researchers - mostly from Europe and the USA - have dealt with the failure modes of sheet metals since the 50s. Lankford [1] and then more researchers [2-11] showed that the anisotropy coefficient (r) and the work-hardening coefficient (n) are strongly related to sheet formability. However, regarding a large number of press-shop measurements carried out by the NADDRG (North American Deep-drawing Group), the correlations do not enable us to answer Pierce's [12] questions: "what mechanical properties are required satisfactory to produce a certain pressing trouble-free? Furthermore, when a pressing is running successfully, how close is it to failure?" The answers are in Keeler's publications from the 60s [13, 14], that with the investigation of major and minor principal surface strains in a blank, a limit strain graph could be plotted in biaxial stretching, i.e. from plane strain tension (ε_2=0) up to equibiaxial tension (ε_2=ε_1). Referring the negative strain ratio, Goodwin published a paper in 1968 [15]. Based on these three papers, the Keeler-Goodwin diagram i.e. the forming limit diagram was born. Keeler [16, 17] still proposed the circle grid design as the method of strain measurement, even gave some application examples in the press-shop also. Pearce [18], Kleemola [19], Hecker [20] and Ayres and Brewer [21] worked out the concept that which deformed ellipse (or square) and how should be measured.

Tisza has been also comprehensively studying sheet metal formability and forming limits in the last two decades. His research group carried out the so-called "star specimen" to monitor the FLDs' sensitivity for the effect of the rolling direction [22]. They found more intense sensitivity perpendicular and 45° to the rolling direction. In other paper [23], an automatic evaluation system for determining forming limit diagrams was studied. Finite element simulation results based on automatically defined forming limit curve (FLC) showed good agreement with experimental strain fields in case of stainless steel samples. Furthermore, forming limit prediction at single point incremental sheet forming (SPIF) process was also investigated [24]. They performed a systematic experiment series to find the FLC for both the negative and positive minor strain quadrants. The experimental results showed that the forming limit curve for SPIF represents two straight lines with a negative slope in the positive quadrant and with a positive slope in the negative minor strain range, but both are above the conventional forming limit curve.

The experimental technique worked out by Nakajima [25, 26] is the most popular in FLCs' determinations due to its practicalities. In Hungarian research laboratories, other test methods like Marciniak, hydraulic bulge test, etc. are less widespread. Marciniak's name is rather known because of his physical based theoretical FLC definitions.

Marciniak and Kuczinski [27] proposed that the failure starts with local inhomogeneity, and thus gave the theoretical solution for both sides of the FLCs. Similarly, with the investigation of the physical occurrence of a local necking in the sheet, Swift [28], Hill [29] and Stören and Rice [30] also determined the failure in plane strain under different loading conditions. Swift used the Mises-Hencky yield criterion, and the major stress components to predict the major and minor limit strains with the consideration of the strain-hardening capacity of the metal. Hill predicted the failure in plane strain state (FLC_0 point) equal with the onset of local necking, i.e. with the Nádai strain-hardening exponent. In his solution, a 45° slope straight line predicts the description of the negative quadrant ($-\varepsilon_2$). Stören and Rice deduced FLDs from continuum mechanic equations. Although the FLC_0 point was predicted the same way as Hill did, their new bifurcation method led to new relationships, called vertex theory, in both negative and positive ranges between the major and minor strains. Chow et al. [31] extended later this theory for anisotropic materials.

Among the semi-empirical methods, which main advantage is the easier definition of the necessary material parameters, Keeler and Brazier [32] were one of the firsts who made a comprehensive study about the strain limits from simple properties of materials. They experienced similarity in the geometry refers to FLDs of more material grades. They specified a linear correlation between the FLC_0 point and material parameters – like sheet thickness and strain hardening exponent – and then they assumed a curve shifting along the major strain axis. Similar context can be found in the paper of Cayssilas [33] who already took into consideration the strain rate-hardening exponent, too. He further developed his predicting model more times [34] and validated the results with many experiments at Arcelor Research S. A. Abspoel et al. [35] from Tata Steel Research Development also proposed a method for FLC evaluation from mechanical properties originated from tensile test results. With the investigation of approximately fifty steel grades, they defined a relationship statistically between the total elongation and the major and minor strains at four different strain paths in the FLC. The equations consider the anisotropic behavior and the sheet thickness too. Similarly, from tensile test results, Levy and Tyne [36] deduced the major strains to define stress based forming limit curve, subsequently. They used Hill anisotropic yield criterion to evaluate the FLC_0 i.e. the major strain corresponding to the zero minor strain – and thus identified a linear approximation for both sides of the FLD.

This paper is a review about the observation of different limit strains both theoretically and experimentally for automotive DP steels.

2. Experimental analysing of formability

2.1. Applied materials

Three types of conventional DP steels as DP600, DP800 and DP1000 with the basic mechanical properties according to MSZ EN ISO 6892-1:2010 tensile tests' results, with 30 mm/min displacement velocity were applied in this study. The tensile specimens with gauge length of 80 mm and 1mm thickness were manufactured in three directions: parallel, perpendicular and 45° to the rolling direction (RD). The stress-strain curves in the coordinate system of true (logarithmic) and equivalent quantities and the Lankford coefficients in different directions as the tensile tests' results can be seen in figure 1.

It can be seen that DP steels show nearly isotropic behaviour. Figure 1.b presents the Lankford coefficients in the different directions, which also highlights that the transverse-thickness strain ratios are close to unity. The main mechanical properties are summarized in Table 1, where the $\bar{r}$-value is calculated as:

$$\bar{r} = \frac{r_0 + r_{90} + 2r_{45}}{4} \tag{1}$$

in which r_0, r_{90} and r_{45} denotes the measured values in 0°, 90°and 45° to the rolling direction. In Table 1, Ag belongs to the engineering uniform elongation. The values of strain hardening exponent (n) and the strength coefficient (K) in the Nádai expression (2) are fitted by the least-squares method.

$$\sigma_{eq} = K \cdot \varepsilon_{eq}^{n} \tag{2}$$

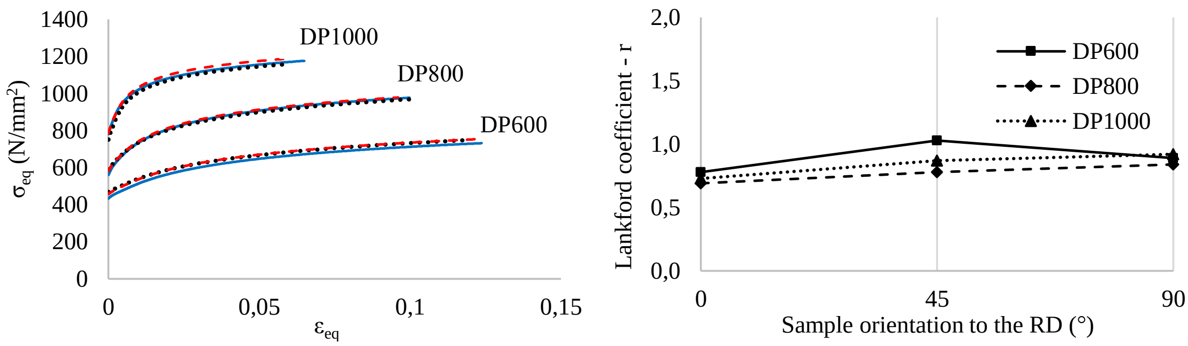

Figure 1. Flow curves of DP600, DP800 and DP1000 materials: continuous line parallel, dashed line perpendicular, dotted line 45° to the RD (a); and Lankford coefficients in 0°, 45° and 90° to the RD (b)

Table 1. Main mechanical properties of the investigated DP steels

	UTS N/mm²	YS N/mm²	A_{80} (%)	Ag (%)	K	n	$\bar{r}$
DP600	656	445	20.6	13.6	918	0.112	0.92
DP800	879	571	16.0	10.8	1217	0.104	0.75
DP1000	1099	767	10.6	7.0	1481	0.083	0.76

2.2. Forming Limit Diagrams

Five different geometries embodied the minimum necessary numbers of samples (figure 2.a) to cover the FLCs from pure shear up to equi-biaxial tension. We used rectangular grids on the sheet surfaces to determine the major (ε_1) and minor (ε_2) logarithmic strains belonging to the onset of local necking. An Erichsen 142 type universal sheet formability tester equipment was applied to form the prepared samples without any lubricant (figure 2.b). It has a practical significance, since the sheet panels carry various oils, such as mill oil, washer oil, and press lubricant in the automotive industry. As a result, the lubrication system become more complicated, and lubrication performance become poorer in the press-shop compared to the laboratory conditions [32]. The stroke speed of the punch was 30 mm/min. The machine automatically stopped itself at the load drop caused by the occurrence of crack.

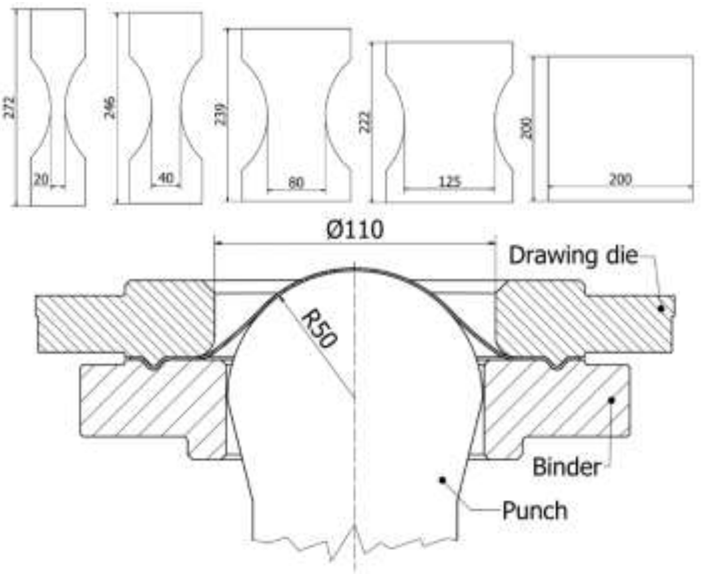

(a)

(b)

Figure 2. Sample geometries with different cross-widths: 20, 40, 80, 125 and 200 mm respectively (a); and the arrangement of tools at the Nakajima test with 100 mm punch diameter (b)

We used Vialux Autogrid® strain-analyzer system in agreement with Mercedes-Benz Manufacturing Hungary Ltd. for the detection of local strains. We adhered to the description of "ISO 12004-2:2008 Determination of forming-limit curves in the laboratory", during the calculation of the limit values. It specifies that the necking strain is equal with the maximum point of the best fit second order inverse parabola curve (3), which is superposed for the strain values in the relevant section containing the neck, see figure 3.a, which illustrates a DP600 sample with 20 mm cross-width. The inner boundaries of the curve fitting are found there, where the second derivative of the measured strains gives the positive maximum at each side of the crack. Figure 3.b shows the major strains as well as the derivative along the section's length.

$$f(x) = \frac{1}{ax^2 + bx + c}, \tag{3}$$

here x denotes the curvilinear length of the sample's cross section, while a, b, c are constants.

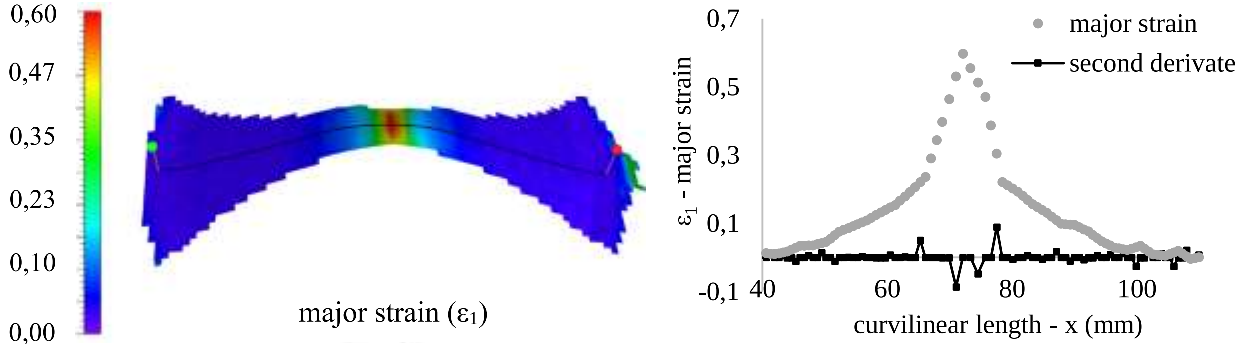

(a) (b)

Figure 3. Strain distribution in a DP600 sample highlighting the relevant section with black line (a); and the measured major strains and those second derivatives (b)

Ignoring the cracked points, the fitted inverse parabola curve can be received, which first derivative is identical with the strain at the onset of local necking: figure 4.a. The measured limit values obtained with this method for the investigated steels and approximated linearly in the coordinate system of the major and minor strains are illustrated in figure 4.b.

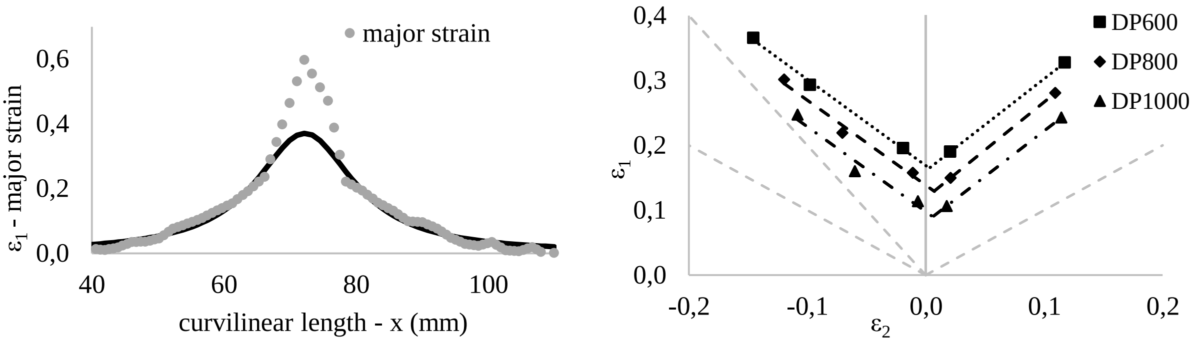

(a) (b)

Figure 4. Major strain points with the fitted inverse parabola curve (a); experimentally defined limit strains and the forming limit curves of the investigated steels (b)

3. Theoretical FLC prediction

Though the theoretical FLC prediction models disregard the effect of the friction, some of them are in good agreement with the experimental results in the negative quadrant of the FLC and in plane strain tension.

Hill assumed that the necessary criterion of local necking is the occurrence of plane strain state in the sheet ($d\varepsilon_2 = 0$). Consequently, his solution does not allow the localized necking for biaxial stretching, i.e. when $\varepsilon_2 > 0$. According to his equations (4), the FLC_0 point is equivalent with the strain-hardening exponent (n) and thus the limit major strain (ε_1*) increases linearly with a slope of -1 in the negative quadrant. Comparing the left hand side of the FLC points given by his method with the experiments, it can be observed that the experimental curves have more powerful slope than the theoretical ones (figure 5). It is visible in figure (b), that the slopes exceed one third the -1 value for all steels. Besides, the FLC_0 points are obviously under predicted by Hill.

$$\varepsilon_1{}^* = \frac{n}{1+\rho} \qquad -1 < \rho \le 0 \tag{4}$$

where ρ means the strain ratio

$$\rho = \frac{\varepsilon_2}{\varepsilon_1} \tag{5}$$

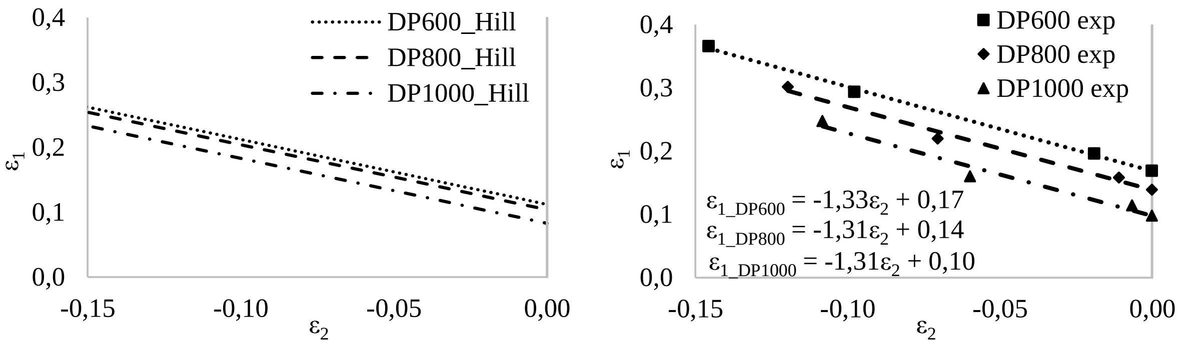

(a) (b)

Figure 5. Major and minor limit strains belonging to the localized necking in Hill's theory (a); and to the experiments (b)

It is generally noticed that the investigated evaluation models somewhat predict under the plane strain point and the left hand side in the FLCs, however are relatively close to the experiments. Meanwhile, the calculated values spectacularly under predict the right hand side of the experimental FLCs due to the friction. The curves in both sides have steeper rising in ε_1 direction caused by the poor lubricant and produce earlier failure considering the minor strain values. It can be seen in figure 6 also, where the evaluated FLC by Swift and the experimental strain data are listed respectively.

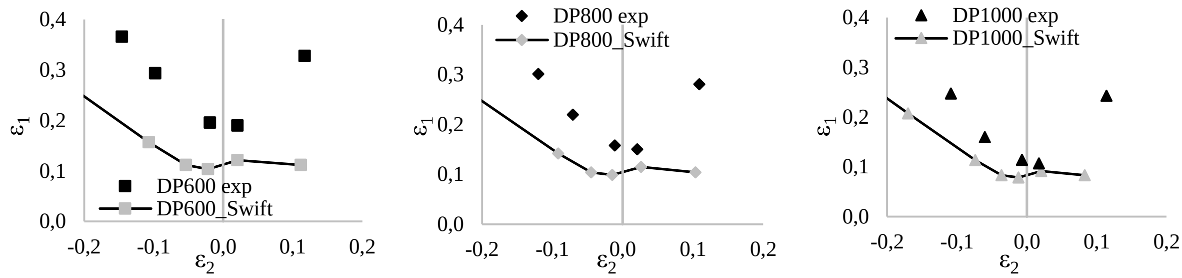

(a) (b) (c)

Figure 6. Major and minor limit strains belonging to the localized necking in Swift's theory (continuous line) and to the experimental strain points for DP600 (a), DP800 (b) and DP1000 (c) shown by the signs of measured points

Based on Swift's and Hill's works, Stören and Rice developed a new bifurcation method, which approximated the FLC with second order and root functions. Based on their description, when $\rho \geq 0$ ($\varepsilon_2 \geq 0$) the FLC curves can be more precisely predicted as the neck forms along the direction of the minimum principal strain. For $\rho < 0$ ($\varepsilon_2 < 0$), the neck inception along the direction of zero extension results their calculation close to Hill's and Swift's theories (figure 7).

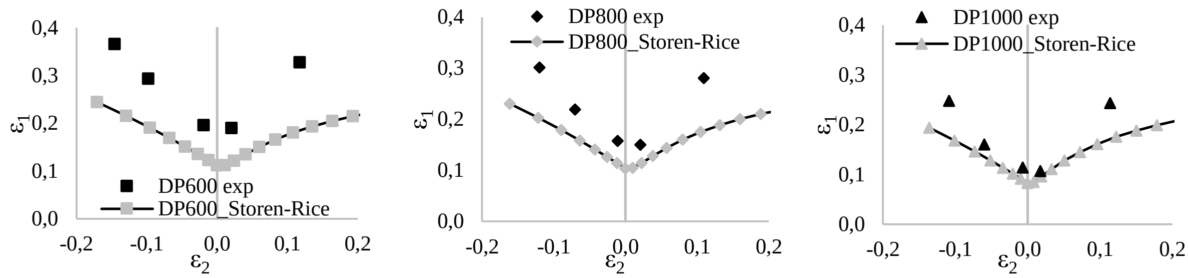

(a) (b) (c)

Figure 7. Major and minor limit strains belonging to the localized necking in Stören and Rice's theory (continuous line) and to the experimental strain points for DP600 (a), DP800 (b) and DP1000 (c)

In North America, FLCs for mild steels, high strength steels (HSS) and advanced high strength steels (AHSS) have been studied and approximated by the Keeler-Brazier method based on the initial sheet thickness (t) and the strain-hardening exponent (n) of the material. The Keeler-Brazier equations (6, 7, 8) are strongly recommended for the prediction of AHSS materials, and as it is visible in figure 8, the evaluated curves are very close to the measured points in the negative range of ε_2, and in plane strain, where the effect of the friction is less significant due to the sample geometries. At the right to ε_1, this model also under predict under the poor lubricant experiments naturally.

$$\mathrm{FLD_0} = \ln\left[1 + \frac{(23.3 + 14.13t)\cdot n}{0.21}\right] \qquad \mathrm{n} \leq 0.21 \tag{6}$$

$$\varepsilon_1{*} = \ln\left[0.6(e^{\varepsilon_2{*}} - 1)\right] + e^{FLD_0} \qquad 0 < \varepsilon_2{*} \tag{7}$$

$$\varepsilon_1{*} = FLD_0 - \varepsilon_2{*} \qquad \varepsilon_2{*} < 0 \tag{8}$$

IOP Conf. Series: Materials Science and Engineering **426** (2018) 012005 doi:10.1088/1757-899X/426/1/012005

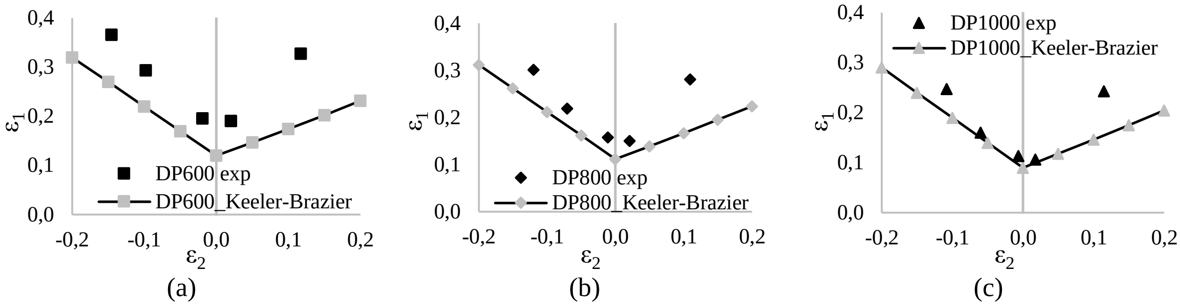

Figure 8. Major and minor limit strains belonging to the localized necking in Swift's theory (continuous line) and to the experimental strain points for DP600 (a), DP800 (b) and DP1000 (c)

Levy and Tyne got the strain data in plane strain from tensile tests' results with using the Hill '48 plasticity assumption (9) and the fact that the logarithmic, axial uniform strain (ε_{crit}) is identical with ε_1* if ε_2 is equal to zero. According to their theory, the negative side of the FLCs can be predicted by a linear assumption with a slope -1 (45°) line based on Hill's solution. Experimental FLCs available from Levy and Green [37] showed that the average slope of the positive side is close to 0.53 for HSLA and DP steels. If ε_{crit} is determined from a given hardening law (2), FLD_0 is obtained by (9, 10), and for any values of ρ, ε_1 and ε_2 can be calculated from the slope values (figure 9).

$$\varepsilon_{eq} = \varepsilon_{crit} = \frac{1+\bar{r}}{\sqrt{(1+2\bar{r})}}\sqrt{\varepsilon_1^2 + \varepsilon_2^2 + \frac{2\bar{r}}{1+\bar{r}}\varepsilon_1 \cdot \varepsilon_2} \tag{9}$$

$$\varepsilon_1{*} = \varepsilon_{crit} \qquad if \qquad \varepsilon_2 = 0 \tag{10}$$

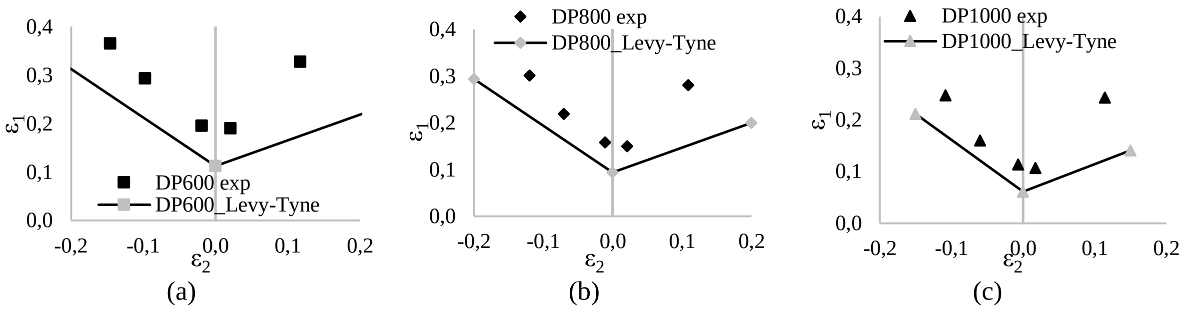

Figure 9. Major and minor limit strains belonging to the localized necking in Swift's theory (continuous line) and to the experimental strain points for DP600 (a), DP800 (b) and DP1000 (c)

It is worth mentioning that the predicted curves according to the Levy-Tyne theory are also closer to the measured data at the left hand side than at the right.

4. Conclusion

Results of different theoretical methods for predicting the FLC were compared to the experimental curves for DP600, DP800 and DP1000 steels. Although friction has important effect, the experiments were carried out without any lubricant and the effect of the friction have not been also examined.

Despite the enhanced friction, many theories are relatively close to the left hand side of the experimental FLC. This is due to the fact, that most evaluations in the negative minor strain range or accept Hill's solution either be close to it, which slope is only differs with one-third to the experiments. Furthermore, at the DP800 and DP1000 steels, the predicted curves almost totally overlap the measured strains in plane strain tension. The effect of the friction can be rather observed in the positive quadrant of the FLDs, where the contact areas are larger between the samples and the punch.

IOP Conf. Series: Materials Science and Engineering **426** (2018) 012005 doi:10.1088/1757-899X/426/1/012005

Acknowledgement
This research is supported by EFOP-3.6.1-16-2016-00014 project. The Project is supported by the Hungarian Government and co-financed by the European Social Fund.

References
[1] Lankford W I, Snyder S C, Bauscher J A. 1950. *Trans. ASM* **42** pp 1196-1232
[2] Sowerby R, Johnson W 1975. *Mat. Sci. Eng.* **20** pp 101-111
[3] Mellor P B, Parmar A 1978. *Mechanics of sheet metal forming. Material behavior and deformation analysis* (New York/London, Plenum Press) pp 53-57
[4] Mellor P B 1982. *Mechanics of materials* ed Hopkins G (Oxford, Pergamon Press) pp 383-415
[5] Chatfield D A, Keeler S P 1971. *Technology for using sheet steel designing for formability*, (Metal Progress), pp 60-63
[6] Banabic D, Dorr R I 1992. *Formability of thin sheet metals* (Romania), Bucarest, O. I. D. I. C. M.
[7] Whiteley R L 1960. *Trans. ASM* **52** pp 154-157
[8] Hill R 1950. *The mathematical theory of plasticity* (Oxford, Clarendon Press)
[9] Hosford W F, Backofen W A 1964. *Fundamentals of deformation processing* (Syracuse University Press) pp 259-292
[10] Warwick J O, Alexander J 1962/63. *J. Ins. Met.* **91** pp 1-10
[11] Fukui S, Yoshida K, Abe K 1960. *Sci. Papers Inst. Phys. Chem. Res.* **54** pp 199-205
[12] Pearce R 1991. *Sheet metal forming*, (Adam Hilger Series on new manufacturing processes and materials, IOP Publising Ltd)
[13] Keeler S P 1965. *Society of Automotive Engineers* No. 650535
[14] Keeler S P, Backofen W A 1963. *Trans. ASM* **56** pp 25-48
[15] Goodwin G M 1968. *Society of Automotive Engineers* No. 680093, pp 380-387
[16] Keeler S P 1968. *Circle Grid Analysis* (Livonia, MI: National Steel Corporation)
[17] Keeler S P 1968. *Society of Automotive Engineers* No. 680092
[18] Painter M J, Pearce R 1974. *J. Phys. D: Appl. Phys.* **7** p 992
[19] Kleemola H J, Kumpulainen J O 1980. *J. Mech. Work. Tech.* **3** p 289
[20] Hecker S S 1974 *Met. Eng. Q.* **14** p 30
[21] Ayres R A, Brewer E G 1979. *Society of Automotive Engineers*, No. 790741
[22] Tisza M, Kovács P Z, Lukács Z, Kiss A, Gál G 2015. *Materials Science Forum* **812** pp 271-275
[23] Kovács P Z, Tisza M 2008. *Materials Science Forum* **589** pp 233-238
[24] Tisza M, Kovács P Z and Lukács Z 2012. *Key Engineering Materials* **504-506** pp 863-868
[25] Nakajima K, Kikuma T 1971. *Yamata Technical Report* **284** pp 678-680
[26] Nakajima K, Kikuma T, Hasuka K 1972. *Yamata Technical Report* **264** p 141
[27] Marciniak Z, Kuczynski K 1967. *Int. J. Mech. Sci.* (Pergamon Press) **9** pp 609-620
[28] Swift H W 1952. *Journal of the Mechanics and Physics of Solids* **1** pp 1-18
[29] Hill R 1952. *J. Mech. Phys. Solids* **1** p 19
[30] Stören S, Rice J R 1975. *J. Mech. Phys. Solids* (Pergamon Press) **23** pp 421-441
[31] Chow C L, Jie M, Hu S J 2003. *Journal of Engineering Materials and Technology* **125** (Transactions of the ASME)
[32] Altan T, Tekkaya A E 2012. *Sheet Metal Forming Fundamentals*, (ASM International OH 44073 0002) pp 44-51
[33] Cayssials F 1999. *Proc. IDDRG Congress Brussel*, pp 443-454
[34] Cayssials F, Lemoine X 2005. *Proc. IDDRG Congress Besançon*, pp 1-8
[35] Abspoel M, Scholting M E, Droog J M M 2013. *Journal of Materials Processing Technology* **213** pp 759–769
[36] Levy B S, Van Tyne C J 2015. *Proc. IDDRG Shanghai*, pp 262-269
[37] Levy B S, Green D E 2002. *Analysis and Documentation of Laboratory Studies on the Enhanced FLC Concept* (Auto/Steel Partnership, Southfield, MI, USA)